Article

Biotribological Characteristic of Peanut Harvesting Impact-Friction Contact under Different Conditions

Peng Zhang [1,2], Hongbo Xu [1,3,*], Xiaoru Zhuo [1,4], Zhichao Hu [5,*], Chenglong Lian [6] and Bing Wang [1]

[1] Nanjing Institute of Agricultural Mechanization, Ministry of Agriculture and Rural Affairs, Nanjing 210014, China; zhangpeng01@caas.cn (P.Z.); xrzhuo@hhu.edu.cn (X.Z.); wangbing@caas.cn (B.W.)
[2] College of Engineering, Nanjing Agricultural University, Nanjing 210031, China
[3] College of Engineering, China Agricultural University, Beijing 100083, China
[4] College of Mechanics and Materials, Hohai University, Nanjing 210098, China
[5] Key Laboratory of Modern Agricultural Equipment, Ministry of Agriculture and Rural Affairs, Nanjing 210014, China
[6] College of Forestry, Shandong Agricultural University, Taian 271018, China; lyjj917@sdau.edu.cn
[*] Correspondence: xuhongbo@caas.cn (H.X.); huzhichao@caas.cn (Z.H.); Tel.: +86-(0)25-84346251 (H.X.)

Abstract: Although cutting flow peanut-picking is the main peanut harvesting method, it has the problems of a large harvest loss and a high damage rate of peanut shells. The analysis of impact-friction contact characteristics during peanut fruit picking is crucial to illustrate peanut fruit picking damage. A typical peanut variety, "Dabaisha", was considered in this study. The characteristics of peanut-picking impact-friction were studied using a peanut-picking impact-friction test bench under different conditions. An orthogonal test with three factors and levels was performed after the single-factor condition was determined. The apparent morphologies of peanut shells before and after the collision and friction tests were compared and analyzed using micro-computed tomography, white-light interferometry, and optical microscopy, whereas the impact-friction damage characteristics of peanuts under the influence of various factors were discussed. The results show that the orders of influence of the coefficient of friction of peanuts and wear loss of peanut pods were as follows: invasion depth > moisture content > contact linear velocity and moisture content > invasion depth > contact linear velocity, respectively. The experimental results and discussion in this study can provide a data reference for developing and designing peanut mechanization production equipment.

Keywords: peanut harvest; contact damage; coefficient of friction; wear loss; orthogonal test

1. Introduction

Peanut is one of the most important cash and oil crops, and it occupies a paramount position in global oil production and trade [1,2]. With the restructuring of China's planting sector, the planting area of peanuts has increased significantly, accelerating the development of scale production [3,4]. Therefore, it is imperative to realize an efficient mechanized peanut harvest. The design theory and method of key components of peanut harvesting are inadequate, and the performance parameters of shell picking systems cannot completely adapt to the production conditions in China [5,6]. In particular, effective research methods for gaining insight and analyzing local physical phenomena, such as contact displacement and impact force in the peanut harvester shell picking process, are still lacking [6]. The research and development (R&D) technology reserve of and investment in peanut harvesting machinery are insufficient because the equipment accuracy is not high. Reduction of the damage rate in shell picking and transportation has always been critical in developing peanut mechanization harvesting technology [7]. The loss caused by collision damage accounts for approximately 15% of the annual total loss. The impact damage to peanuts during harvesting, processing, and transporting is a crucial factor for maintaining the quality and economic value of peanuts [6,8,9]. Most of the peanut harvesting is carried out

in two steps in harvesting operations in China. This first involves digging out the peanuts from the soil to dry them using a peanut digger, then the dried peanuts are collected and harvested using a combine. The types of peanut picking are divided into axial flow and tangential flow, which have similar peanut pod picking characteristics. As shown in Figure 1 (type of tangential flow for peanut picking), peanut seedlings and kernels are fed from the pick-up area and are rotated using a picking drum by grasping and driving via picking spring teeth. Peanut pods break away from the vine and fall through a concave screen to the selected parts due to active forces (strike force, carding-pulling force, and comb-pulling force) from the picking teeth, constraining forces (friction and impact force) from the concave screen, and squeezing and rubbing forces between plants. In addition, peanut plants are discharged from combines, thus completing the fruit picking operation [10–13]. The entire process can be considered a process of picking via continuous collisions and contact between the spring teeth, concave screen, and peanut plants. The peanut shells are mainly damaged by contact forces of various forms, such as collision and extrusion, between the peanut pod, vine, and fruit picking mechanism [12,13]. However, so far only studies of peanut impact damage have been undertaken and no friction collision content has been included [7,10]. In addition, no study investigating the frictional characteristics of peanut harvesting has been reported.
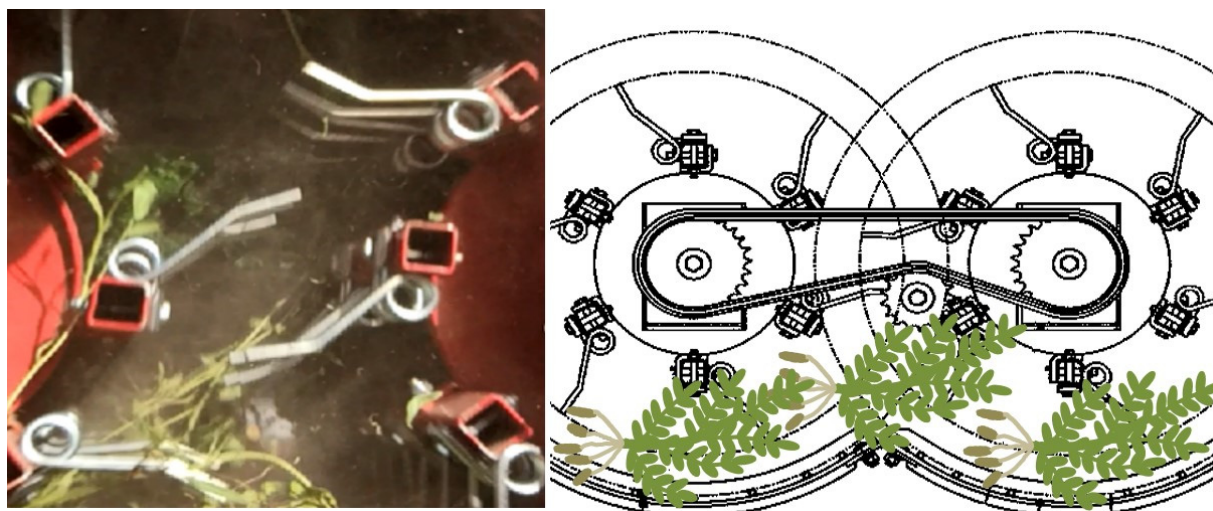

Figure 1. Schematic diagram of the peanut pod picking process.

Since the 19th century, research on the characteristics of grain friction has been ongoing, mainly focusing on the highly mechanized production of rice, wheat, corn, soybean, and other staple crops [14–16]. There are few studies on the frictional mechanical properties of grains in other countries. However, the effects of collision and friction contact characteristics have not been considered. The reported experimental data are unsuitable for direct application in the production practice of mechanized peanut harvesting in China due to several differences in grain varieties [17]. While studying the collision and contact mechanisms for harvesting other crops, Lizhang et al. investigated the impact characteristics of threshing materials from the perspective of threshing damage of corn and wheat and reviewed the research progress of the threshing damage of rice [15,18]. They established the displacement history and maximum pressure distribution equations between rice seeds and threshing elements from the perspective of contact mechanics. In addition, they obtained the critical velocity between rice and the threshing element when rice cracked or broke. Moreover, the influence of moisture content on the impact damage of rapeseed and wheat has been studied [19,20]. Horabik et al. studied the influence of rapeseed on the recovery coefficient of different impact materials based on the viscoelastic Hertz contact model [21]. Dintwa et al. studied the effect of the viscoelastic coefficient of the collision of two apples on their kinetic energy loss [22]. Stropek et al. measured the deformation of apples due

to impact through high-speed projection [16]. They used high-speed cameras, mechanical sensors, and two independent measurement systems to evaluate and estimate the dynamic behavior of the impact on a rigid plate and study the effect of different types of material packaging on the impact damage. The above studies mainly focused on the contact damage theory of various crops, such as corn, soybean, wheat, and apple [15,16,19,20,22,23]. However, the mechanism of the impact damage of peanut harvesting has not yet been studied. The physical properties of the impact of peanuts in different directions have also been mentioned in many studies using a universal testing machine, but the friction coefficient during impact contact has been ignored [24]. Several methods for measuring the coefficient of friction of peanuts have been proposed in other studies, such as the parallel wall method, shear box method, inclined surface method, etc. [25,26]. The coefficient of friction used in many studies of peanut harvesting equipment design is usually measured using the inclined surface method [11–13]. The coefficient of friction measured by this method is simply the coefficient of sliding friction or rolling friction. However, the contact created between the peanut pod and the picking part is friction with impact during the picking process.

In this study, a peanut-picking impact-friction tester was designed to study the impact and friction characteristics of peanuts from harvesting mechanical parts during peanut harvesting. The parameters of shape, size, and friction characteristics of peanuts with different moisture contents were measured using the peanut-picking impact-friction tester. The variations in friction parameters with the moisture content of peanut pods, contact linear velocity, and invasion depth were analyzed. The difference between impact-friction characteristics of peanuts and different contact materials was also investigated. This study provides a reference for the design of peanut harvesting equipment, research on the damage characteristics of biological impact-friction, and a method of parameter measurement.

2. Materials and Methods

2.1. Specimens of Peanut and Pin

Figure 2 depicts peanut and pin specimens. The peanut specimen is "Dabaisha", which is a typical peanut variety from the main peanut-producing areas in China. The specimens were collected randomly during peanut maturation. The parameters of moisture content, surface morphology, and weight were calibrated after collecting the specimens.
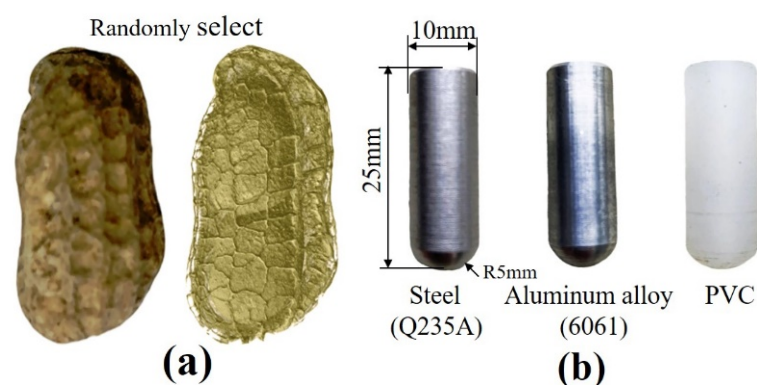

Figure 2. Specimens used in tests: (**a**) peanut and micro-CT-scanned images and (**b**) photographs of pin specimens of different materials.

The two-step process for peanut harvesting is the main harvest method in China. Peanut plants are dug out of the ground for drying first, then collected for peanut picking and cleaning (separation of plant and pod) by combine, thus completing the peanut harvesting.

Full-feed peanut harvesting involves digging, drying, and picking peanuts using peanut combines. The average moisture contents of peanuts for two, three, and four days were 33.8%, 24.5%, and 16.7%, respectively. Therefore, the moisture content of the peanut for testing was set according to the three intervals of 14~16%, 24~26%, and 34~36%. To

obtain peanut specimens with different moisture contents, the specimens with the required moisture content were prepared following the drying method of Yan et al. [27] and the moisture content measurement standard of the national standard [28]. Hiscan XM micro-computed tomography (Micro-CT) (Suzhou Hiscan Information Technology Co., Ltd., Suzhou, China) was employed to record the three-dimensional (3D) scanning of peanut pods, which was used to compare the surface damage characteristics of peanuts after the experiment. The X-ray tube settings were 60 kV and 133 µA, and images were acquired at 70 µm resolution. A rotation step of 0.5° through a 360° angular range with a 50 ms exposure per step was used. A scanning white-light interferometer (SWLI) (Taylor Hobson, Leicester, UK) was used to observe the surface morphology of the contact area of the pin. A 0.25 mm cutoff with a 10 × objective, 0.3 numerical apertures, and 1 × scanning speed in the XYZ mode (512 × 512 resolution) were used.

The peanut specimens were cleaned with a brush before the experiment to prevent the soil carried on the surface of the peanuts from contributing to contact processes such as impact and friction. All specimens were weighed and labeled after preparation, placed in double-layered sealed bags, and stored in a refrigerator at 26 °C for future use. A schematic of a peanut specimen used in the test is shown in Figure 2a. Mechanical picking contact part (pin) specimens were made of Q235A steel, 6061 aluminum alloy, and PVC. The size of the pin specimens was 10 mm, and they were processed according to the diameter of the peanut fruit picking spring tooth. To effectively measure the collision and friction contact during fruit picking, the contact end of the pin specimens was processed as a semicircle with a 10 mm diameter. A schematic of a pin specimen used in the test is shown in Figure 2b.

2.2. Peanut-Picking Impact-Friction Tester

In this study, a peanut-picking impact-friction tester was designed to examine the peanut-picking mechanism of peanut harvesting under different conditions. Figure 3 shows a schematic and photograph of the tester. The main working parts are the control computer, 1000 W Servo motor (DELTA, ECM-B3M-E21310RS1, Taipei, Taiwan), motor drive (ASD-B3-1021-L, Taipei, Taiwan, dynamic torque sensor (MRN-01) (range: 0 ± 20 Nm; accuracy: $<\pm0.5\%$), support bearing seat, picking rotary disk, picking spring teeth, peanut specimens, peanut fixed platform, 3D force sensor (SZOBTE, China (CL-TR5S) X: 5/200 N, Y: 5/200 N, Z: 5/200 N), lifting platform, and other parts. The driving shaft was driven by a servomotor to achieve positive and negative rotations and stable speed output under fixed torque to ensure the accuracy of test conditions. The driving shaft transmits power to the rotary disk through the torque sensor, and the connecting part is connected by coupling. The rotary disk was held in place by a bearing support to avoid vibrations or eccentricity due to the impact force in the test process. The peanut specimen was fixed on the platform, and its height could be adjusted by lifting. The power output by the motor drives the pin to rotate and contact with the fixed peanut to produce impact-friction. The fixing claw was coated with silica gel (thickness: 2 mm) to keep the surface of peanut intact when the peanut specimen was being fixed. The dynamic torque sensor was connected to the driving shaft to measure the spindle torque (T). A 3D force sensor was mounted under the specimen holder to measure the variation in triaxial force (F_x, F_y, F_z). The control and parameter settings of the experiment were realized using Labview programming. Dynamic curves of coefficients of friction and period changes can be identified in the display. The coefficient of friction (μ) was calculated using the measured force, as follows:

$$\mu = \frac{\frac{T}{r}}{\sqrt{F_z{}^2 + F_x{}^2 + F_y{}^2}} \tag{1}$$

where r denotes the turning radius and F_x, F_y, and F_z are the applied load forces in the x-, y-, and z-directions, respectively.

(1) Control PC; (2) Servo motor; (3) Fixed support of motor; (4) Coupling; (5) Torque sensor; (6) Center bearing bracket; (7) Pin holder; (8) Pin; (9) Peanut sample; (10) Peanut holder; (11) Three-dimensional force sensor; (12) Lifting platform; (13) Power switch.

(a)

(1) PC; (2) Servo motor; (3) Coupling; (4) Torque sensor; (5) Center bearing bracket; (6) Test part; (7) Pin holder; (8) Pin; (9) Peanut sample; (10) Peanut holder; (11) 3D force sensor; (12) Lifting platform; (13) Power switch.
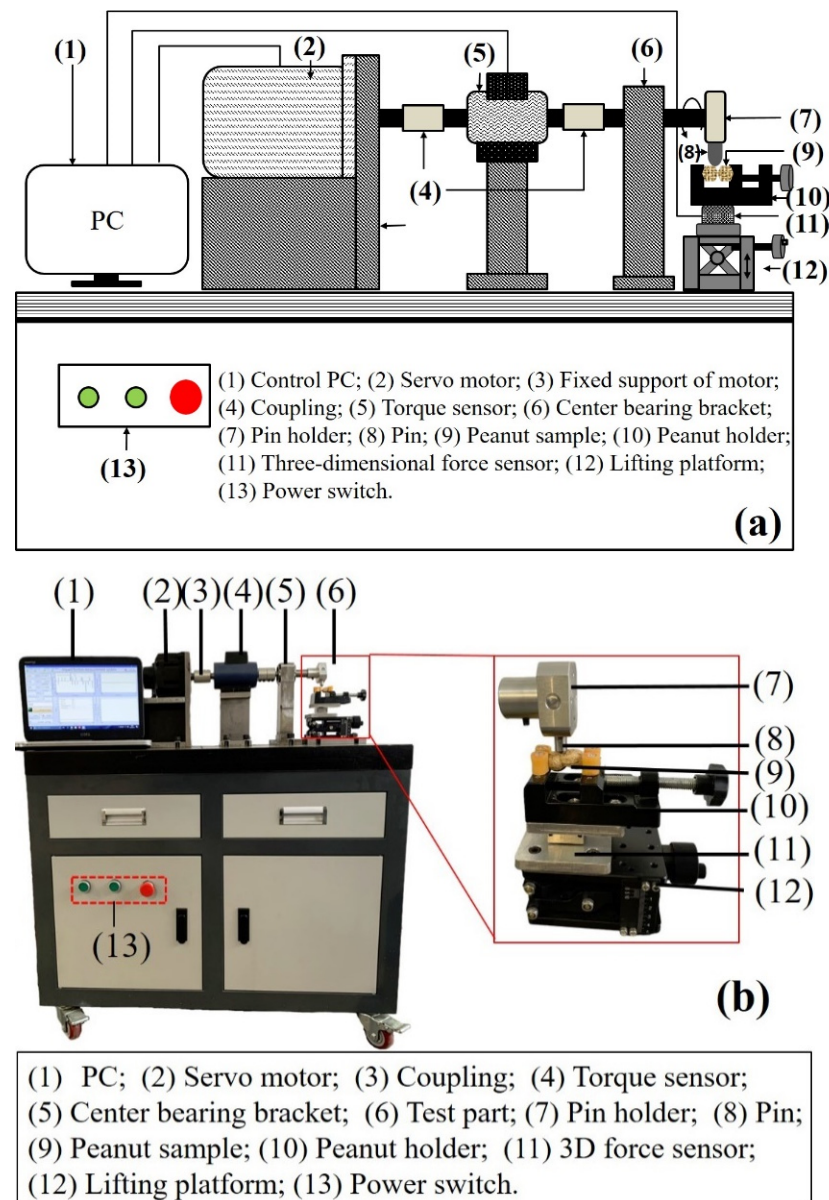
(b)

Figure 3. (**a**) Schematic and (**b**) photograph of the designed peanut-picking impact-friction tester.

2.3. Test Conditions and Methods

In this study, the main exposure conditions of peanuts during harvesting were considered. In particular, the variation characteristics of the surface of the peanut shell after impact-friction were investigated under three conditions: moisture content, invasion depth, and contact material type. The test bench's speed of 1500 rpm was calculated according to the contact linear velocity (9.8 m/s) of the peanut-picking drum rotating at 274 rpm. Therefore, the contact linear velocity was set to 5, 10, and 15 m/s. Because the moisture content of peanuts at the time of harvest was between 15% and 35%, the moisture level was set to 15%, 25%, and 35% in the experiment. Invasion depths of 1, 2, and 3 mm were set for the impact-friction test. Three types of contact materials (Q235A steel, 6061 aluminum alloy, and PVC) were selected to be processed into pin specimens and compared with peanut in the experiment. All single-factor tests were performed with median values, which were set as 10 m/s, 25%, 2 mm, and Q235A steel. Table 1 lists the details of the conditions for the impact-friction test.

Table 1. Experimental conditions.

Parameters	Values
Contact linear velocity (m/s)	5/10/15
Moisture content (%)	15/25/35
Materials used for pin specimens	Q235A steel/6061 aluminum alloy/PVC
Invasion depth (mm)	1/2/3
Initial temperature (°C)	26
Cycle of impact contact	72,000
Variety of peanut	Dabaisha

A multifactor orthogonal test was performed to investigate the three factors (contact linear velocity, moisture content, and invasion depth), which significantly influence the coefficient of friction and wear loss of the peanut pods. The effects of the three factors and three horizontal conditions on the coefficient of friction and wear loss were investigated based on the Box–Behnken experimental design principle [29]. The experimental scheme included 17 experiments, comprising 12 analysis factors and 5 zero errors. The test data were analyzed by quadratic polynomial regression using Design-Expert software (STAT-Ease Inc., Minneapolis, MN, USA). The correlation and interaction effects among different factors were analyzed using response surface analysis.

The pin specimens were ultrasonically cleaned thoroughly with acetone before each test. The soil on the surface of the peanut was cleaned with high-pressure air currents to ensure the consistency of the surface of the peanut specimens in each test. To investigate the surface wear morphology of pin specimens after collision friction, optical microscope (OM) and SWLI micrographs are shown to identify the wear mechanisms involved.

2.4. Surface Contact Analysis of Impact-Friction

The mechanical properties of peanuts are related to the moisture content; peanuts are brittle and plastic when the moisture content is low and high, respectively. To simplify the theory, the peanut specimen was regarded as a brittle material because it was harvested after drying until its moisture content was low.

The collision and friction processes between the peanut and picking part can be divided into two stages: elastic deformation and damage. The stress distribution in the contact zone during the elastic deformation stage can be derived from the quasistatic Hertz theory [30,31]. When the elastic deformation reaches the maximum deformation, the peanut is damaged, forming a stress crack or breakage [21,30]. A schematic of the contact and wear areas is shown in Figure 4. The coefficient elliptic equations are as follows:

$$A = \frac{1}{2R_1} \tag{2}$$

$$B = \frac{1}{2}\left(\frac{1}{R_1} + \frac{1}{R_2}\right) \tag{3}$$

where A and B denote the coefficients of the elliptic equations of the contact area of the pin and peanut specimens, respectively, and R_1 and R_2 denote the radius of the pin and peanut specimens, respectively.
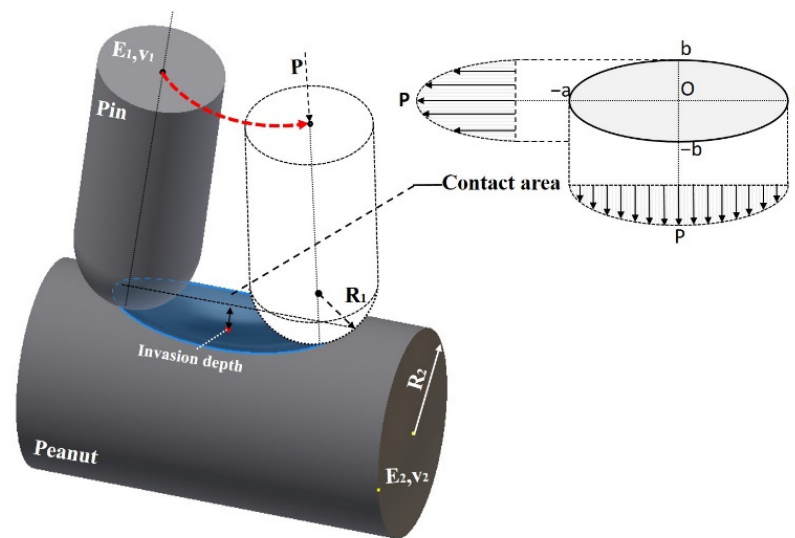
Figure 4. Schematic of the contact and wear areas.

The dimensions of the contact surface can be expressed as follows:

$$a = 1.145n_1 \sqrt[3]{F \frac{R_1 R_2}{(R_1 + 2R_2)} \left(\frac{1 - v_1^2}{E_1} + \frac{1 - v_2^2}{E_2} \right)} \tag{4}$$

$$b = 1.145n_2 \sqrt[3]{F \frac{R_1 R_2}{(R_1 + 2R_2)} \left(\frac{1 - v_1^2}{E_1} + \frac{1 - v_2^2}{E_2} \right)} \tag{5}$$

where a and b denote the long and short axes of the ellipse contact surface, respectively. n_1 and n_2 denote the coefficient of Hertzian contact stress deformation [32]. F represents the normal load, E_1 and E_2 denote Young's modulus of the pin and peanut specimens, respectively, and v_1^2 and v_2^2 denote Poisson's ratio of the pin and peanut specimens, respectively.

The types of forces mainly affecting peanuts during fruit picking are impact force and friction force. The maximum compressive stress (σ_{Max}) [30] of peanut shell due to collision is

$$\sigma_{Max} = 0.365n_3 \sqrt[3]{\frac{F \left(\frac{R_1 + 2R_2}{R_1 R_2} \right)^2}{\left(\frac{1 - v_1^2}{E_1} + \frac{1 - v_2^2}{E_2} \right)^2}} \tag{6}$$

The center of the two objects is close to the displacement due to elastic deformation during the collision and friction between the peanut and picking part. The contact relative displacement (δ) is estimated as follows:

$$\delta = 0.665n_4 \sqrt[3]{F^2 \frac{(R_1 + 2R_2)}{R_1 R_2} \left(\frac{1 - v_1^2}{E_1} + \frac{1 - v_2^2}{E_2} \right)^2} \tag{7}$$

The maximum shear stress (τ_{Max}) due to friction is calculated as follows:

$$\tau_{Max} = \sigma_{max} \times f \tag{8}$$

Suppose that the yield compressive stress of a peanut shell is σ_s, the peanut shell is destroyed under compression when $\sigma_{max} > \sigma_s$, which is the condition of peanut shell impact failure.

When τ_{Max} is greater than the adhesion between the pin and peanut shell or the yield shear stress (τ_s) of the peanut shell, the peanut shell peels or rubs off under the action of friction, which is the condition of peanut shell friction damage.

The τ_s of peanut shells increases with increasing yield compressive stress of peanut shells. Therefore, the extent to which impact or friction damages the peanut shell depends on the ratio of σ_{max} to σ_s.

3. Results and Discussion

3.1. Single-Factor Experimental Evaluation

3.1.1. Materials of Pin

The test results show the effect of a single factor on the coefficient of friction. Figure 5 shows the effect of different materials on the coefficient of friction of the peanut shell surface. All aspects of material parameters influence the coefficient of friction of peanut shells. The coefficient of friction differs for different materials due to different hardness, strength, plasticity, and toughness of the materials. PVC is weaker than the other two materials in resisting material surface pressure. However, the coefficient of friction exhibits a relatively stable change during collision and friction with the peanut. The coefficient of friction of iron and aluminum is small; however, it shows varying degrees of fluctuation due to peanut shell surface tissue damage during collision.
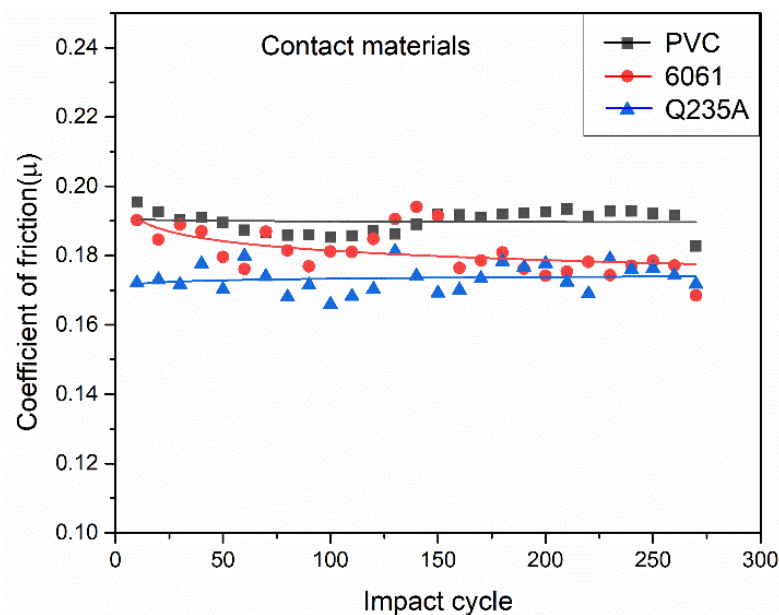

Figure 5. Changes in the coefficient of friction depending on different materials of pin specimens.

The worn-out surfaces of the pins of different materials were observed using an OM and an SWLI (Figure 6). As PVC has a weaker ability to resist pressure than Q235A steel and 6061 aluminum alloy, surface deformation and fatigue spalling occur during the collision and friction with peanuts, thereby leading to severe surface wear. This is the direct reason for the largest friction coefficient of PVC materials among the three materials.

The aluminum surfaces also exhibited fine wear patterns during the test. However, the surface wear of iron remained almost unchanged. However, one side appeared higher than the other side on the contact surface due to the attachment of the residue of peanut surface tissue to the surface of the pin after the collision and friction with the peanut. This is also the reason for reducing the friction coefficient of Q235A steel, because peanut shell tissue and moisture participate in the friction process.
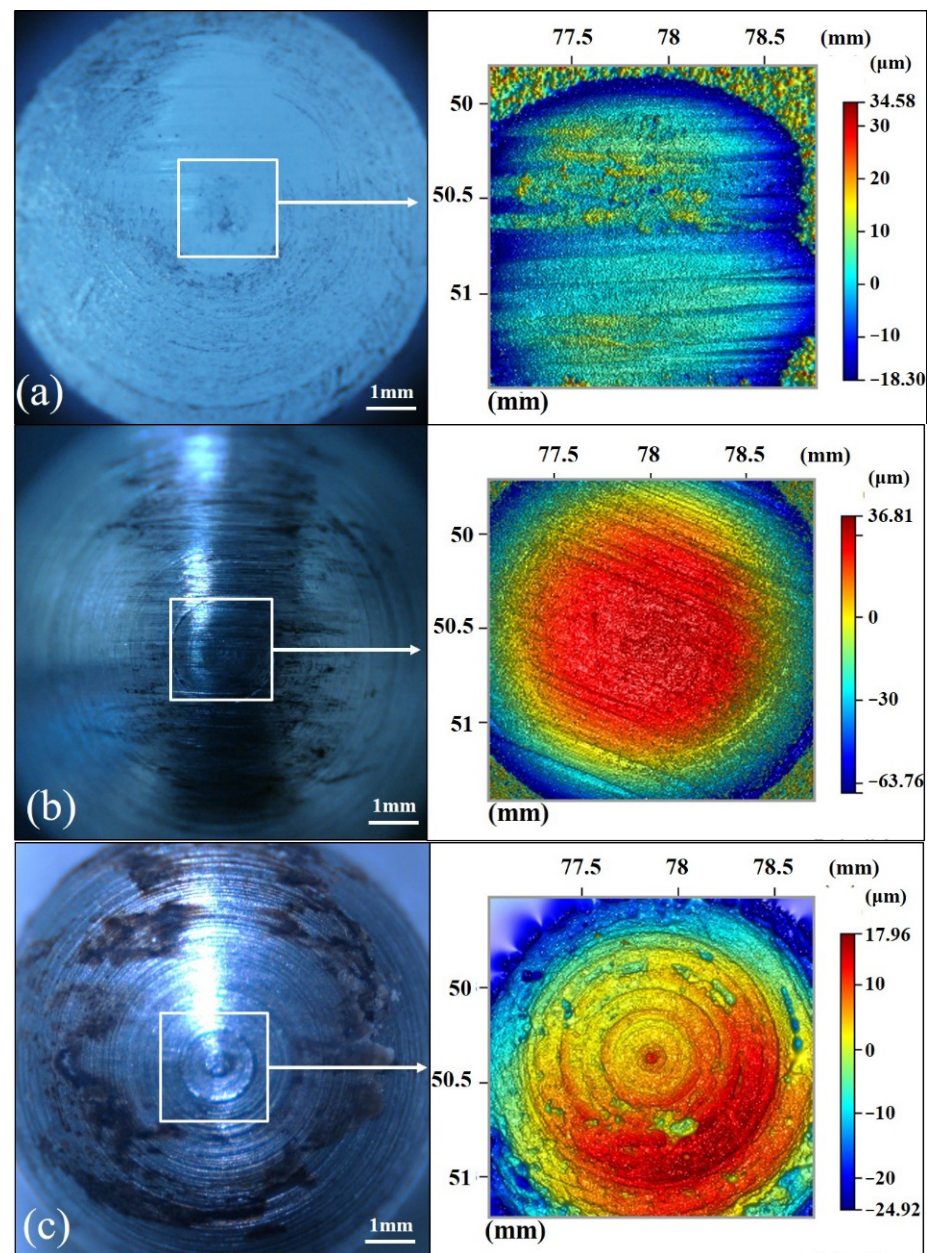
Figure 6. Optical microscopy surface and three-dimensional surface topography images of the pin specimens with different materials: (**a**) PVC, (**b**) 6061 aluminum alloy, and (**c**) Q235A steel.

3.1.2. Contact Linear Velocity

The plot of the influence of different contact linear velocities on the coefficient of friction of the peanut shell's surface is shown in Figure 7. The contact linear velocity affects the coefficient of friction, presenting an inverse relationship between the peanut and pin during the contact process. The friction coefficient of peanut is between 0.16 and 0.19 when the contact linear velocity is in the range 5–15 m/s. The coefficient of friction shows a difference before 60 cycles of impact contact, which is almost similar when the contact linear velocity is 5 and 10 m/s. However, the coefficient of friction at a contact speed of 10 m/s decreases gradually after 60 cycles because the surface morphology of the pin and peanut shell in the early stage of collision contact changes slightly. The tissue of the peanut contact surface starts to sustain damage, whereas the wear of the pin contact surface and other factors affect the change in the coefficient of friction after a critical point of approximately 60 cycles. Similarly, the coefficient of friction of the friction pair shows a decreasing trend after 10 cycles and tends to stabilize after 40 cycles when the contact speed condition is

15 m/s. Compared with the contact linear velocity conditions of 5 and 10 m/s, fluctuations appear earlier in the coefficient of friction when the contact linear velocity is 15 m/s. This indicates that an increase in the contact linear velocity in the contact friction between the peanut shell and pin accelerates the appearance of contact surface damage so that the friction pair can reach a stable contact state as soon as possible. These factors also affect the coefficient of friction.
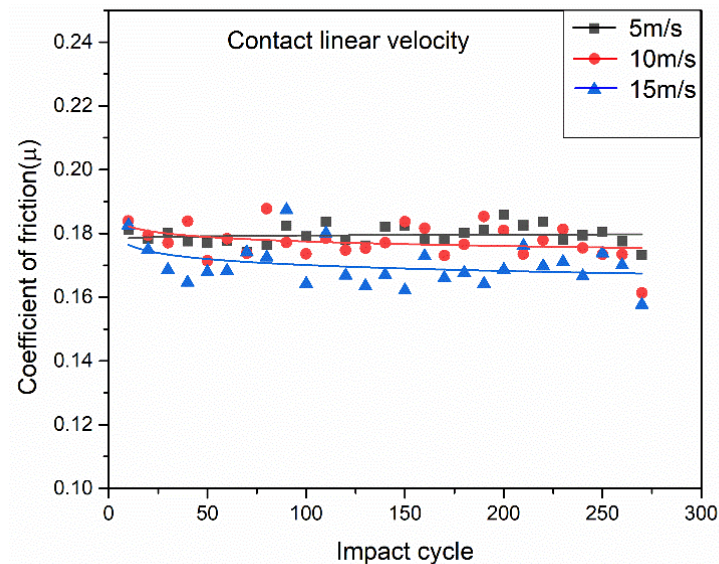

Figure 7. Changes in the coefficient of friction depending on different contact linear velocity of pin specimens.

3.1.3. Contact Invasion Depth

Figure 8 shows the plot of the influence of different invasion depths on the coefficient of friction of the peanut shell's surface. The results show that the friction coefficient of peanut is between 0.17 and 0.19 when the contact invasion depth is in the range 1–3 m/s. The coefficient of friction shows the maximum value when the invasion depth of the pin on the surface of the peanut shell is 2 mm and the fluctuation amplitude is the maximum. The coefficient of friction of the pin tends to be the most stable when the invasion depth of the pin on the contact surface of the peanut shell is 1 mm. The fluctuation behavior of the coefficient of friction is the most severe when the invasion depth of the pin on the surface of the peanut shell is 3 mm. It increases from 20 to 40 cycles, at which it reaches its maximum and then decreases to the coefficient of friction of the invasion depth of 1 mm. This shows that the damage rate of peanut shell surface tissue accelerates and the change in the coefficient of friction is affected when the invasion depth is 3 mm.

The effect of the peanut's moisture content on the coefficient of friction is shown in Figure 9. The results show that the friction coefficient of peanut is between 0.15 and 0.21 when the moisture content of peanut is in the range 15–35%. The coefficient of friction decreases with increasing the peanut's moisture content because the moisture in the peanut shell is transferred to the contact surface during the contact process, which acts as a lubricant to participate in the contact friction behavior. It is also the main factor affecting the change in the coefficient of friction. The coefficient of friction shows a declining trend within 20 cycles and is highly stable when the peanut's moisture content is 35%.
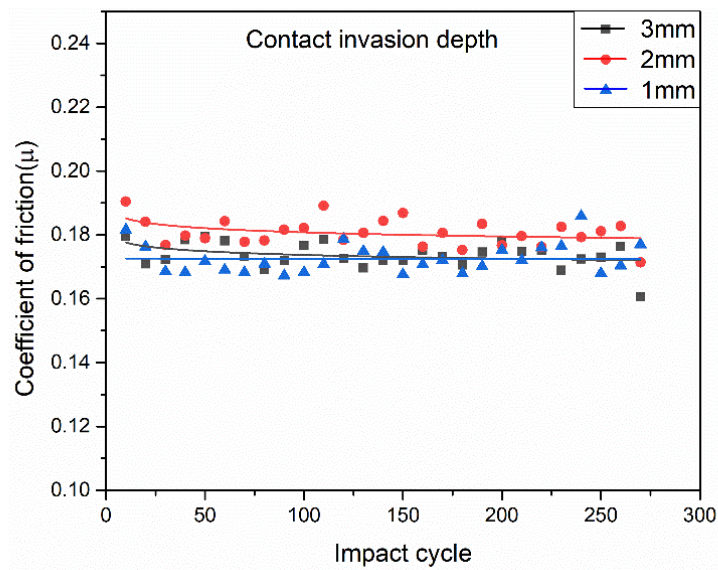
Figure 8. Change in the coefficient of friction depending on the different contact invasion depth conditions.
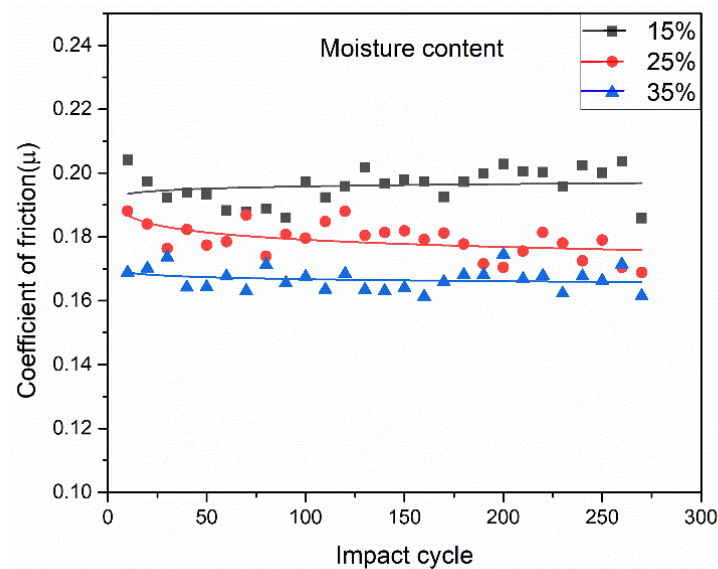
3.1.4. Moisture Content of Peanut

Figure 9. Change in the coefficient of friction depending on the different moisture content conditions.

The worn-out surfaces of the pins of different materials were observed using an OM and an SWLI (Figure 6).

Figure 10 shows the surface morphology of the pin after the peanut impact-friction test under different peanut moisture content conditions. The topography of the contact surface can be clearly observed from the scan image using WSLI, and the color gradient indicates the distribution of the contact surface height from 0 to 50 μm. Figure 10a–c are the surface morphology images (OM and SWLI) under the moisture content conditions of 15%, 25% and 35%, respectively. The surface wear degree of the pin and peanut collision contact is not obvious; however, some peanut tissues are still attached to the pin's surface even after being worn off. The adhesion degree of the peanut tissue on the pin's surface is inversely proportional to the peanut's moisture content. When the moisture content was 15%, the peanut tissue attached to the pin's surface was concentrated in the central part. However, when the moisture content was 25% and 35%, the peanut tissues attached to the pin's surface accumulated to one side due to the impact-friction processes. This indicates that the peanut moisture is involved in the impact-friction behaviors during the

contact between the pin and peanut, which is also the main factor affecting the change in the coefficient of friction.
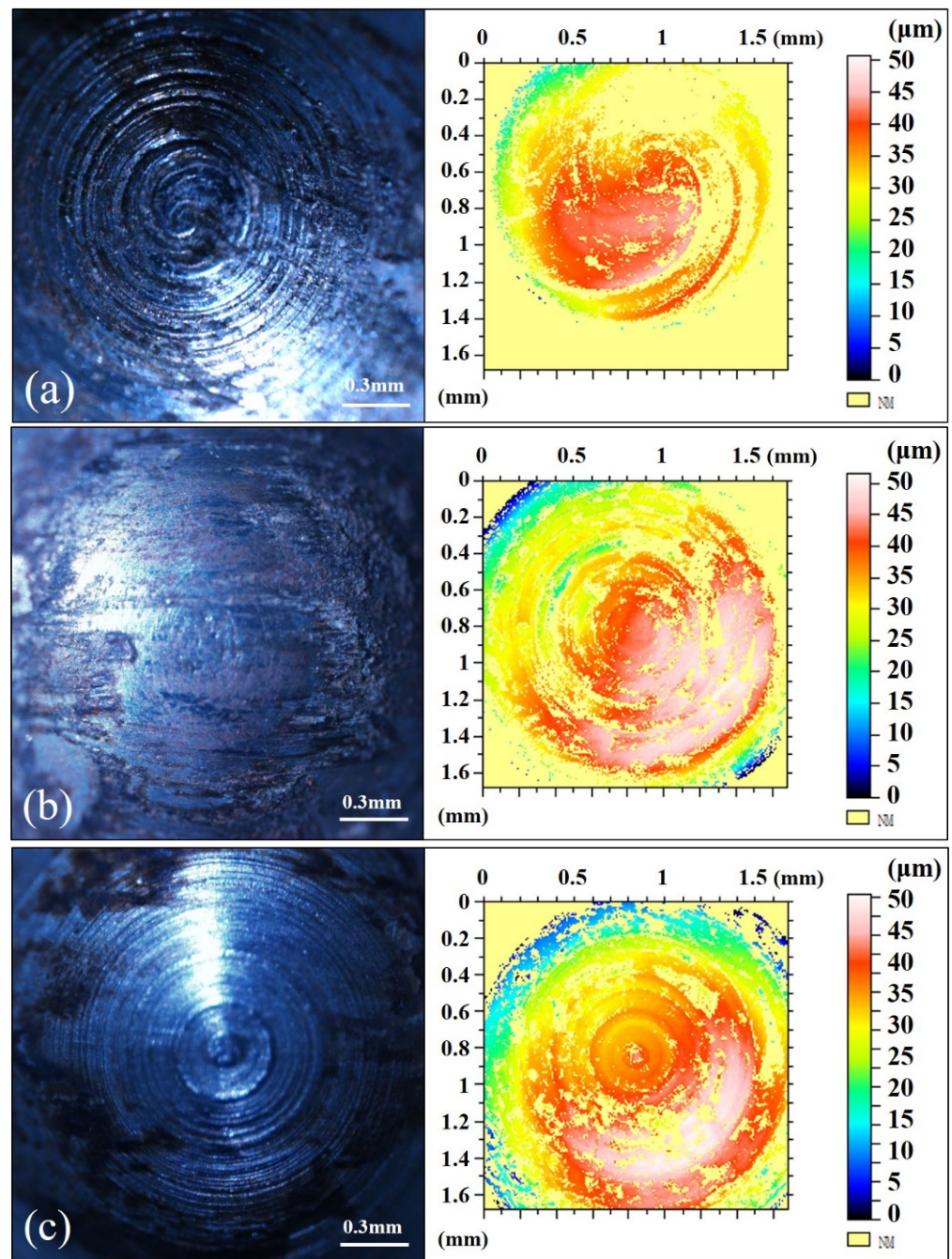

Figure 10. Optical microscopy surface and three-dimensional surface topography images of a pin specimen under different moisture content conditions of the peanut shell: (**a**) 15%, (**b**) 25%, and (**c**) 35%.

The moisture content of crops determines their mechanical properties and rupture strength, which directly affect the damage of peanut shells. It is a critical factor affecting the quality of fruit picking operations. The ability of a peanut with low moisture content to resist damage is small, and the wear situation is mainly brittle spalling.

3.2. Evaluation of Multifactor Orthogonal Tests

3.2.1. Establishment of Regression Model and Significance Test

Multiple regression fitting analyses were performed according to the data specimens in Table 2 to find the optimal working parameters. The quadratic polynomial response surface regression model of the coefficient of friction (Y_1) and wear loss (Y_2) to three independent variables of contact linear velocity (X_1), moisture content (X_2), and invasion depth (X_3) was established. The regression equation was analyzed using analysis of variance (ANOVA), and the results are shown in Table 3. The final equations in terms of actual factors are given by Equations (9) and (10). $p < 0.0001$ for response surface models of Y_1 and Y_2 indicates that the regression model is extremely significant. A lack of fit $p > 0.05$ (0.0531 and 0.1415, respectively) indicates that the regression model has a high fitting degree. The influence of each parameter on regression can be reflected by the value of p. There are two regression terms in the model of Y_1 with very significant influence ($p < 0.01$): X_2 and X_3. There are also two regression items in the model of Y_1 with significant influence ($p < 0.05$): $X_1 \times X_2$ and $X_2{}^2$. In addition, there are three regression terms in the model of Y_2 with very significant influence ($p < 0.01$): X_2, X_3, and $X_3{}^2$. Further, there are two regression items in the model of Y_2 with significant influence ($p < 0.05$): X_1 and $X_2 \times X_3$. The orders of the influence of the three factors on Y_1 and Y_2 are $X_2 > X_3 > X_1$ and $X_1 > X_2 > X_3$, respectively, which can be confirmed by the F values of each factor (Table 3).

$$Y_1 = 0.24 - 0.02X_1 - 0.05X_2 + 0.027X_3 + 0.001X_1X_2 + 0.001X_1X_3 \\ -0.004X_2X_3 - 0.0005X_1{}^2 - 0.0006X_2{}^2 - 0.003X_3{}^2 \tag{9}$$

$$Y_2 = -3.99 - 1.79X_1 + 1.98X_2 + 1.99X_3 + 0.016X_1X_2 - 0.15X_1X_3 \\ -0.6X_2X_3 + 0.12X_1{}^2 - 0.04X_2{}^2 + 24.93X_3{}^2 \tag{10}$$

Table 2. Multifactor experimental design and response values for peanut impact-friction experiment.

No.	Contact Linear Velocity X_1 (m/s)	Moisture Content X_2 (RH%)	Invasion Depth X_3 (mm)	Coefficient of Friction Y_1 (μ)	Wear Loss Y_2 ($\times 10^{-5}$ mm³)
				Response Values	
1	10	25	2	0.185	85.64
2	10	35	1	0.168	21.42
3	10	25	2	0.187	88.37
4	15	15	2	0.197	98.81
5	15	25	1	0.174	37.79
6	5	35	2	0.171	76.33
7	10	25	2	0.184	89.52
8	10	25	2	0.182	90.13
9	5	15	2	0.208	98.17
10	5	25	3	0.187	198.38
11	5	25	1	0.170	23.64
12	10	35	3	0.173	176.66
13	10	15	1	0.196	31.85
14	10	15	3	0.217	211.22
15	15	25	3	0.194	209.54
16	15	35	2	0.184	80.25
17	10	25	2	0.187	93.21

Table 3. Variance analysis of regression equation for peanut impact-friction multi-factor experiment.

Source	Coefficient of Friction Y_1				Wear Loss Y_2			
	Sum of Squares	Degree of Freedom	F Value	Significant Level (p)	Sum of Squares	Degree of Freedom	F Value	Significant Level (p)
Model	2.772×10^{-3}	9	20.78	0.0003	61,882.99	9	461.23	<0.0001
X_1	2.113×10^{-5}	1	1.43	0.2714	111.53	1	7.48	0.0291
X_2	1.860×10^{-3}	1	125.53	<0.0001	911.43	1	61.14	0.0001
X_3	4.961×10^{-4}	1	33.47	0.0007	57,987.15	1	3889.74	<0.0001
X_1X_2	1.440×10^{-4}	1	9.72	0.0169	2.69	1	0.18	0.6838
X_1X_3	2.250×10^{-6}	1	0.15	0.7084	2.24	1	0.15	0.7101
X_2X_3	6.400×10^{-5}	1	4.32	0.0763	145.56	1	9.76	0.0167
X_1^2	5.329×10^{-6}	1	0.36	0.5677	38.73	1	2.60	0.1510
X_2^2	1.580×10^{-4}	1	10.66	0.0138	67.94	1	4.56	0.0702
X_3^2	2.901×10^{-5}	1	1.96	0.2045	2616.97	1	175.54	<0.0001
Residual	1.038×10^{-4}	7			104.35	7		
Lack of fit	8.575×10^{-5}	3	6.35	0.0531	74.10	3	**3.27**	**0.1415**
Pure error	1.800×10^{-5}	4			30.26	4		
Total	2.876×10^{-3}	16			61,987.34	16		

Note: $p < 0.01$: very significant and $p < 0.05$: significant.

3.2.2. Analysis of the Influence of Interaction Factors on the Coefficient of Friction

The response surface curves of the influence of contact linear velocity, moisture content, and intrusion depth on the response value of Y_1 are shown in Figure 11a–c. Figure 11a shows the interaction response surface diagram of Y_1 between the moisture content of the peanut pod and the contact linear velocity when the invasion depth is 2 mm at the center. A decrease in Y_1 can be realized by increasing the moisture content of the peanut pod and decreasing the collision contact linear velocity. Figure 11b depicts the response surface diagram of the interaction between the peanut surface's invasion depth and contact linear velocity of collision to Y_1 when the moisture content of the peanut pod is 25% at the center. The index of Y_1 decreases with decreasing the peanut surface's invasion depth and contact linear velocity of collision (Figure 11b). Figure 11c shows the response surface diagram of the interaction between the peanut surface's invasion depth and the peanut pod's moisture content to Y_1 when the contact linear velocity of the collision is 10 m/s at the center position. The invasion depth of the peanut pod's surface and the moisture content of the peanut pod significantly influence Y_1; Y_1 decreases with decreasing invasion depth and increasing peanut pod moisture content. The overall impact trend is as follows: Y_1 decreased with decreasing contact linear velocity of collision and invasion depth of the peanut pod's surface, whereas it increased with decreasing moisture content of the peanut pod. The contact area between the peanut pod and picking spring tooth decreased with decreasing the peanut surface's invasion depth, which effectively reduced the damage degree of the peanut shell's surface tissue.

3.2.3. Analysis of the Influence of Interaction Factors on Wear Loss

The response surface curves of the influence of contact linear velocity, moisture content, and intrusion depth on the response value of Y_2 are shown in Figure 11d–f. Figure 11d shows the interaction response surface diagram of the moisture content and contact linear velocity to Y_2 when the invasion depth is 2 mm at the center. A decrease in Y_2 can be realized by increasing the moisture content of the peanut pod and decreasing the contact linear velocity of the collision. However, the impact contact linear velocity on Y_2 is insignificant. Figure 11e depicts the response surface diagram of the interaction between the invasion depth and contact linear velocity on Y_2 when the moisture content of the peanut pod is 25% at the center. Y_2 decreases with decreasing invasion depth and contact linear velocity. Figure 11f shows the response surface diagram of the interaction between the invasion depth and moisture content on Y_2 when the contact linear velocity is 10 m/s

at the center. Y_2 is significantly affected by the invasion depth of the peanut's surface and the moisture content. Y_2 decreases with decreasing invasion depth of the peanut's surface and increasing moisture content. Y_2 is directly proportional to the invasion depth and contact linear velocity and inversely proportional to the moisture content. The primary and secondary relationships are as follows: invasion depth > moisture content > contact linear velocity. This is because the contact area between the peanut pod and pin decreases with decreasing invasion depth. Reducing the contact area between the peanut pod and pin effectively reduces the damage degree of the peanut shell surface tissue and Y_2. The moisture in the peanut shell is involved in the collision contact process and plays the role of a lubricant when the moisture content of the peanut pod increases. It also increases the toughness of the peanut shell, which is not easily damaged. In contrast, the impact contact linear velocity of fruit picking has no significant effect on Y_2.
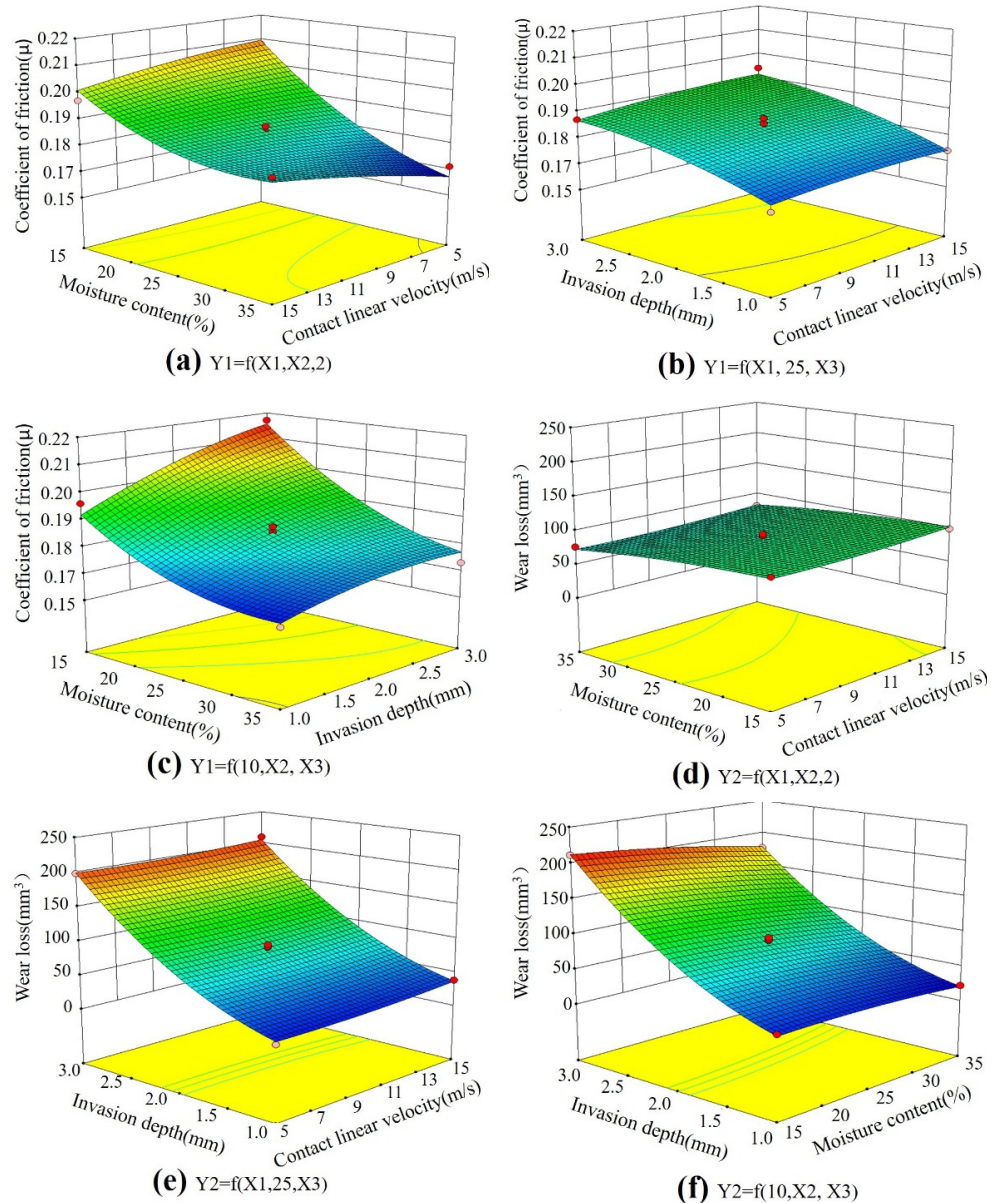

Figure 11. Effects of interactive factors on the coefficient of friction ((**a**) $Y_1 = f(X_1, X_2, 2)$, (**b**) $Y_1 = f(X_2, 5, X_3)$, (**c**) $Y_1 = f(10, X_2, X_3)$) and wear loss ((**d**) $Y_1 = f(X_1, X_2, 2)$, (**e**) $Y_1 = f(X_2, 5, X_3)$, (**f**) $Y_1 = f(10, X_2, X_3)$).

3.2.4. Characterization of Impact-Friction Damage on Peanut Pod

Tomography using micro-CT was used to observe the damage degree of peanut shells after the impact-friction experiment. Figure 12 shows the micro-CT-scan images

of the peanut cross-section. Figure 12(1–17) depict the scan images after the orthogonal test Nos. 1–17, respectively. The original diagram of the sash and crosscut scanning of peanuts is shown in Figure 12(18). The crosscut is a section stretching along the maximum diameter of the worn part of the peanut pod's surface. Peanut pod tissue is divided into exocarp, mesocarp, and endocarp (Figure 12(18)). The morphology of peanut pod tissue was used to judge the wear and damage degree of peanut after the orthogonal test. The damage of peanuts was divided into four grades: abrasion, collapse, cracking, and breaking. Figure 12(1), (3), (7), (8) and (17) show the phenomenon of surface collapse and slight cracking on the surface of peanut shells when the test conditions are all taken as intermediate values (contact linear velocity is 10, moisture content is 25, and invasion depth is 2) and the average wear rate is 89.298 mm^3. The coefficient of friction for this condition ranges from 0.182 to 0.187. This range of friction coefficients can be used as a critical point for peanut shell damage in peanut harvesting equipment and simulation analysis. In Figure 12(10), (12), (14) and (15), the peanut pod tissues are severely damaged with pod loss, and their Y_2 is within 150–200 mm^3. In Figure 12(14), the wearing of the peanut shell tissue occurs when the moisture content is at least 15%. The lower the moisture contents of the peanut pods, the greater the brittleness of their shells. Their ability to resist damage is smaller, and the wear situation is mainly brittle spalling. This is because the peanut shell mainly comprises cellulose and crude fiber. The gap between the peanut kernel and shell increases with decreasing the peanut's moisture content. The surface deformation of the peanut shell decreases with increasing brittleness.
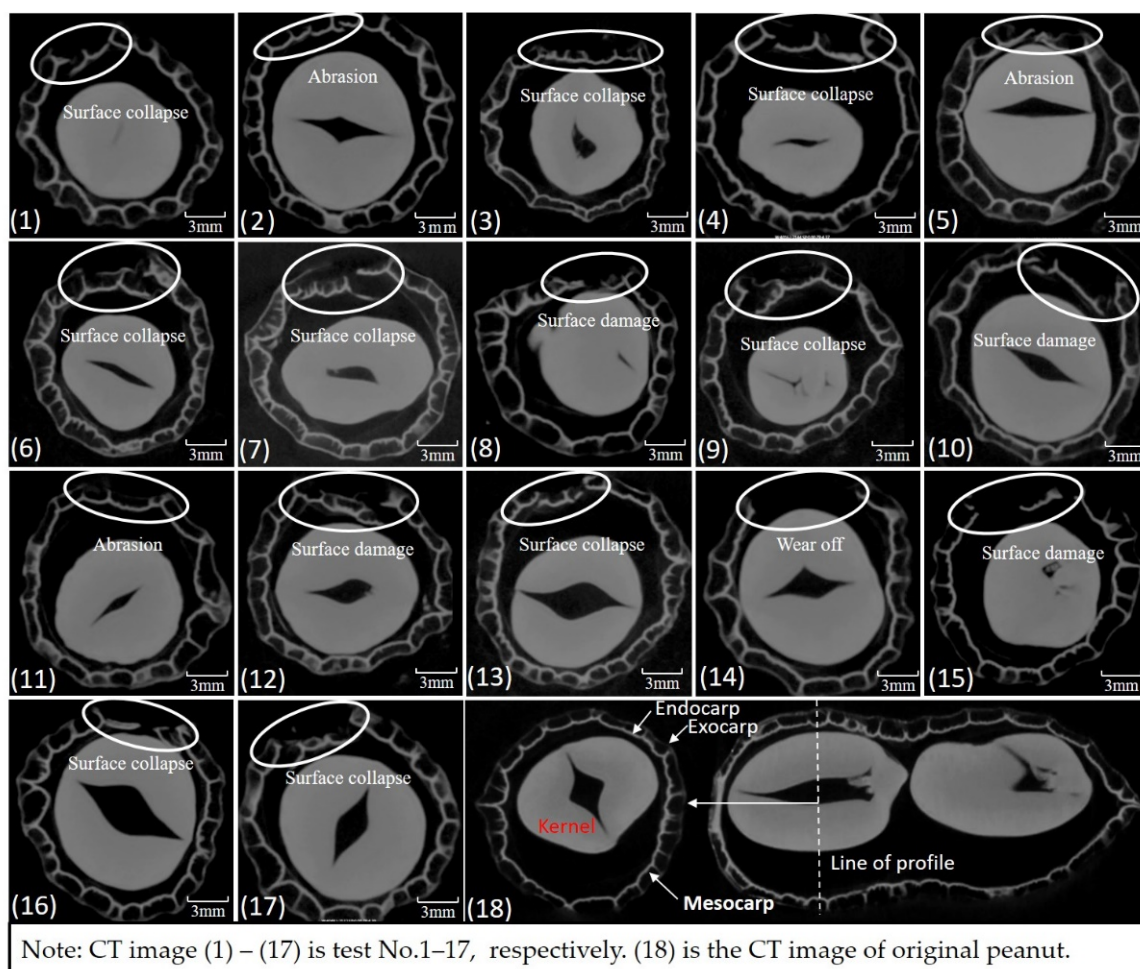

Note: CT image (1) – (17) is test No.1–17, respectively. (18) is the CT image of original peanut.

Figure 12. Micro-CT scan images of peanut cross-section. (**1–17**) are the scan images after the orthogonal test and (**18**) is the scan image before the orthogonal test.

4. Conclusions

The impact-friction and wear characteristics of peanut and pin specimens were investigated using a peanut-picking impact-friction tester in this study. The effects of various factors on peanut impact-friction and wear characteristics were evaluated using an orthogonal test with three factors and levels. The picking parts of different materials have a certain influence on the peanut impact-friction. The hardness, strength, plasticity, and toughness of the materials lead to differences in the coefficient of friction. The relationship between the friction coefficient of peanuts and different materials is PVC (about 0.19) > 6061 aluminum alloy (about 0.18) > Q235A steel (about 0.17). From the point of view of friction coefficient alone, the Q235A steel is suitable for peanut picking parts.

The surface tissue composition and moisture of peanut are involved in biological friction behavior and are also the direct factors affecting friction and wear. In the process of peanut shell and pin contact friction, an increase in the contact linear velocity accelerates the appearance of contact surface damage and makes the friction pair reach a stable contact state as soon as possible. The invasion depth increases the contact area between the pin and peanut shell, accelerating the brittle damage of the peanut shell's contact surface and shedding of the fiber tissue. It also makes peanut shells show different coefficients of friction during the surface tissue shedding. Moisture content is the most significant factor affecting the friction coefficient of peanuts. The moisture in the peanut shell also plays a role in the friction process, affecting the change in the coefficient of friction. The order of influence of the contact linear velocity, invasion depth, moisture content, and other factors on the coefficient of friction of peanuts is as follows: invasion depth > moisture content > contact linear velocity. The friction coefficient of peanut is between 0.15 and 0.21 when the moisture content of peanut is in the range 15–35%. The moisture content of peanuts is a key factor affecting the friction coefficient. The most prominent influence on wear loss is the invasion depth. The range of friction coefficient (0.182~0.187) can be used as a critical point for peanut shell damage in peanut harvesting equipment and simulation analysis. Therefore, a coefficient of friction below 0.182 is helpful for the efficiency of peanut picking. In this study, the biotribological characteristics of peanut and pin were evaluated via impact-friction tests under different conditions. The relevant content and results of this study can provide references for the study of the biotribological characteristics of agricultural crops and the design of peanut harvesting or hulling equipment, and also provide a new method for the impact-friction test that is similar to the peanut picking operation.

References

1. Anco, D. *Peanut Money-Maker 2021 Production Guide*; South Carolina State Library: Columbia, SC, USA, 2021.
2. Fletcher, S.M.; Revoredo, C.L. *World Peanut Market: An Overview of the Past 30 Years*; University of Georgia: Athens, GA, USA, 2009.
3. Shang, S.Q.; Liu, S.G.; Wang, F.Y.; Jang, Y.Z.; Hua, W.J.Y.H. Current situation and development of peanut production machinery. *Trans. Chin. Soc. Agric. Mach.* **2005**, *36*, 143–146.
4. Chen, Y.; Hu, Z.; Wang, H. Restrictive factors and development countermeasure for peanut mechanized harvesting in China. *China Agric. Mech.* **2012**, *4*, 14–17.
5. Gao, L.; Chen, Z.; Charles, C. Development course of peanut harvest mechanization technology of the United States and enlightenment to China. *T CSAE* **2017**, *33*, 1–9.
6. Chen, Z.; Gao, L.; Chen, C.; Butts, C.L. Analysis on technology status and development of peanut harvest mechanization of China and the United States. *Trans. Chin. Soc. Agric. Mach.* **2017**, *48*, 1–21.
7. Hou, J.; Bai, J.; He, T.; Li, J. Damage mechanism of collision contact and applied study progress in typical agricultural materials. *J. Jilin Agric. Univ.* **2020**, *42*, 103–112.
8. Azmoodeh, M.A.; Abdollahpoor, S.; Navid, H.; Moghaddam, V.M. Comparing of Peanut Harvesting Loss in Mechanical and Manual Methods. *Int. J. Adv. Biol& Biomendi Res.* **2014**, *5*, 1475–1483.
9. Stamatov, S.; Ishpekov, S.; Dallev, M. Losses at mechanized harvesting of Bulgarian peanut varieties. Series à Agronomy. *AgroLife Sci. J.* **2020**, *26*, 210–213.
10. Cao, M.; Hu, Z.; Zhang, P.; Yu, Z.; Ye, J.; Wang, S. Key technology of full-feeding peanut picking by tangential flow method. *Int. Agric. Eng. J.* **2019**, *28*, 43–49.
11. Hu, Z.; Wang, B.; Yu, Z.; Peng, B.; Zhang, Y.; Tan, L. Design and test of semi-feeding test-bed for peanut pod picking. *T CSAE* **2017**, *33*, 42–50.
12. Wang, B.; Hu, Z.; Peng, B.; Zhang, Y.; Gu, F.; Shi, L.; Gao, X. Structure operation parameter optimization for elastic steel pole oscillating screen of semi-feeding four rows peanut combine harvester. *T CSAE* **2017**, *33*, 20–28.
13. Lü, X.L.; Hu, Z.C.; Peng, B.L. Analysis and Research on the Picking Roller of the Half-Feed Peanut Combine Harvester. *Appl. Mech. Mater.* **2014**, *597*, 502–506. [CrossRef]
14. Arshad, M.S.; Farooq, M.; Asch, F.; Krishna, J.S.; Prasad, P.V.; Siddique, K.H. Thermal stress impacts reproductive development and grain yield in rice. *Plant Physiol. Biochem.* **2017**, *115*, 57–72. [CrossRef] [PubMed]
15. Xu, L.; Li, Y.; Ding, L. Contacting Mechanics Analysis during Impact Process between Rice and Threshing Component. *T CSAE* **2008**, *24*, 146–7149.
16. Stropek, Z.; Gołacki, K. A new method for measuring impact related bruises in fruits. *Postharvest Biol. Technol.* **2015**, *110*, 131–139. [CrossRef]
17. Güzel, E.; Akçali, I.; Mutlu, H.; Ince, A. Research on the fatigue behavior for peanut shelling. *J. Food Eng.* **2005**, *67*, 373–378. [CrossRef]
18. Xu, L.; Li, Y.; Ma, Z.; Zhao, Z.; Wang, C. Theoretical analysis and finite element simulation of a rice kernel obliquely impacted by a threshing tooth. *Biosyst. Eng.* **2013**, *114*, 146–156. [CrossRef]
19. Szwed, G.; Lukaszuk, J. Effect of rapeseed and wheat kernel moisture on impact damage. *Int. Agrophys.* **2007**, *21*, 299–304.
20. Wojtkowski, M.; Pecen, J.; Horabik, J.; Molenda, M. Rapeseed impact against a flat surface: Physical testing and DEM simulation with two contact models. *Powder Technol.* **2010**, *198*, 61–68. [CrossRef]
21. Horabik, J.; Beczek, M.; Mazur, R.; Parafiniuk, P.; Ryżak, M.; Molenda, M. Determination of the restitution coefficient of seeds and coefficients of visco-elastic Hertz contact models for DEM simulations. *Biosyst. Eng.* **2017**, *161*, 106–119. [CrossRef]
22. Dintwa, E.; Van Zeebroeck, M.; Ramon, H.; Tijskens, E. Finite element analysis of the dynamic collision of apple fruit. *Postharvest Biol. Technol.* **2008**, *49*, 260–276. [CrossRef]
23. Lu, Y.G.; Wu, N.; Wang, B. Measurement and analysis of peanuts' restitution coefficient in point-to-plate collision mode. *J. China Agric. Univ.* **2016**, *21*, 111–118.
24. Yang, R.; Xu, Y.; Shang, S.; Sun, T.; Li, G. Tests and analyses of mechanical properties of peanut root, stem and nut node in mechanical harvest. *Trans. Chin. Soc. Agric. Eng.* **2009**, *25*, 127–132.
25. Akcali, D.; Ince, A.; Guzel, E. Selected physical properties of peanuts. *Int. J. Food Prop.* **2006**, *9*, 25–37. [CrossRef]
26. Gojiya, D.; Dobariya, U.; Pandya, P.; Gojiya, K. Studies on Physical Properties of Peanut Seed. *Acta Sci. Agric.* **2020**, *4*, 1–5. [CrossRef]
27. Yan, J.; Xie, H.; Wei, H.; Wu, H.; You, Z. Optimizing the drying parameters of a fixed bed with reversing ventilation for peanut using computer simulation. *Int. J. Agric. Biol. Eng.* **2021**, *14*, 255–266. [CrossRef]
28. Moisture Measurement—Peanuts. American Society of Agricultural and Biological Engineers: St. Joseph, MI, USA, 2020.
29. Ferreira, S.L.C.; Bruns, R.E.; Ferreira, H.S.; Matos, G.D.; David, J.M.; Brandão, G.C.; da Silva, E.G.P.; Portugal, L.A.; dos Reis, P.S.; Souza, A.S.; et al. Box-Behnken design: An alternative for the optimization of analytical methods. *Anal. Chim. Acta* **2007**, *597*, 179–186. [CrossRef]
30. Knothe, K. *Contact Mechanics and Friction: Physical Principles and Applications*; SAGE Publications Sage: London, UK, 2011.
31. Yang, X.; Qian, S.; Chu, Y.; Liu, S. The calculation method of Hertzian and non-Hertzian contact theory. *J. Huangshan Univ.* **2017**, *19*, 13–18.
32. Cooper, D.H. Hertzian Contact-Stress Deformation Coefficients. *J. Appl. Mech.* **1969**, *36*, 296–303. [CrossRef]